LIMNOLOGY
and
OCEANOGRAPHY

ASLO

Limnol. Oceanogr. 9999, 2025, 1–14

doi: 10.1002/lno.70063

RESEARCH ARTICLE

Large sediment methane production potential in reservoirs compared to lakes and rivers

Pascal Bodmer,[1,2,a] Christoph Bors,[1] Liu Liu,[3*] Andreas Lorke[1]

[1]Institute for Environmental Sciences, University of Kaiserslautern-Landau, Landau, Germany; [2]Département des Sciences Biologiques, Groupe de Recherche Interuniversitaire en Limnologie, Université du Québec à Montréal, Montreal, Canada; [3]Yunnan Key Laboratory of Plateau Geographical Processes and Environmental Change, Faculty of Geography, Yunnan Normal University, Kunming, China

Abstract

Inland waters emit a globally significant amount of methane (CH_4) into the atmosphere. Measurements of potential CH_4 production rates in the sediment can help constrain the magnitude of CH_4 sources and time-averaged emission rates. We explored the magnitude, variability, and drivers of potential CH_4 production rates in the sediment, based on compiled measurements (238 sediment cores from 72 aquatic systems) following a standardized laboratory incubation procedure. The data reveal > 4-fold higher potential CH_4 production rates in reservoir sediments than lakes and > 14-fold higher than rivers after being standardized for temperature. Sediment organic carbon content and depth below the sediment–water interface are universal drivers for potential CH_4 production rates across freshwater ecosystems. The disproportional high CH_4 production rate in sediments from human-made water bodies calls for more comprehensive monitoring of their CH_4 emissions to inform carbon footprint and inventory efforts. This first meta-analysis of potential CH_4 production rates in sediments from different types of freshwater aquatic systems may help with process-based modeling of CH_4 emissions from individual water bodies in larger-scale assessments.

The atmospheric concentration of the potent greenhouse gas methane (CH_4) has more than doubled since the preindustrial era and is contributing ~ 23% to the current radiative forcing of climate change (Etminan et al. 2016; Saunois et al. 2020). Recent estimates suggest that inland waters contribute nearly half of the total combined CH_4 emissions from natural and anthropogenic sources (Rosentreter et al. 2021), yet these emissions cause the greatest uncertainty in current CH_4 budgets (Saunois et al. 2020). Major uncertainties arise from the areal and temporal upscaling of fluxes at the air-water interface, which are mostly based on sparse and episodic measurements despite the extensive observational evidence of their large spatial and temporal variability (Bastviken et al. 2011; Deemer et al. 2016; Rosentreter et al. 2021). More accurate estimates of inland water CH_4 emissions and, more importantly, predictions of their response to climate change and anthropogenic stressors, require a better mechanistic understanding of the processes that regulate these emissions.

Methane emitted from freshwater ecosystems is a final product of the decomposition of organic matter by methanogenic archaebacteria in anaerobic environments and is produced mainly in sediments (Bastviken 2009; but *see*, e.g., Bogard et al. 2014; Liu et al. 2024 for oxic CH_4 production in the water column). Methane produced in sediment can be emitted into the atmosphere through diffusive gas exchange at the air–water interface, but also in the form of rising gas bubbles (ebullition) or through macrophytes (Bodmer et al. 2024; Deemer and Holgerson 2021; Stanley et al. 2016). However, large fractions of CH_4 can be oxidized to carbon dioxide (CO_2) when exposed to aerobic conditions or through anaerobic oxidation (Mayr et al. 2020; Reed et al. 2017; Sawakuchi et al. 2016). In shallow aquatic systems, ebullition can efficiently bypass oxidation by transporting CH_4 directly from the sediment to the atmosphere (McGinnis et al. 2006).

---

*Correspondence: liu.liu@ynnu.edu.cn

[a]Present address: Department of Ecology and Evolutionary Biology, Cornell University, Ithaca, NY, USA

Associate editor: John Melack

Data Availability Statement: The data supporting this study are available at https://doi.org/10.18728/igb-fred-944.1.

Despite the large variability and dynamics within individual water bodies and poor predictability by environmental drivers across different water bodies (Bastviken et al. 2011; Rosentreter et al. 2021), the controls on CH_4 emissions were found to depend on waterbody type (Deemer and Holgerson 2021), suggesting important differences in CH_4 dynamics between rivers, lakes, and reservoirs. To a large extent, the strong temporal and spatial variability of CH_4 emissions observed during short-term flux measurements is caused by the physical processes that regulate the CH_4 transport from sediment to the atmosphere. These include the diffusive flux across the sediment–water interface (D'Ambrosio et al. 2022; Sun et al. 2022), vertical and horizontal advection and dispersion within the water body (Bastviken et al. 2008; Encinas Fernández et al. 2016), gas transfer across the air–water interface (Jansen et al. 2020; MacIntyre et al. 1995), as well as the formation and release of gas bubbles in the sediment (Liu et al. 2016; Maeck et al. 2014; Wik et al. 2013). However, at extended time scales, atmospheric emissions are regulated by CH_4 production and oxidation rates.

Methane production in anaerobic sediments is primarily controlled by organic matter quantity and quality, and sediment temperature (Segers 1998; Yvon-Durocher et al. 2014). The production rates have been measured extensively in laboratory incubations of natural sediment samples (e.g., West et al. 2012) and during experiments with organic-matter additions (Grasset et al. 2018). Since under in-situ conditions the production rates can be affected by the dynamic physical and biogeochemical conditions at the sediment–water interface (D'Ambrosio et al. 2022), production rates measured under standardized laboratory conditions can only be considered as potential CH_4 production rates. Close agreement between temperature-corrected potential CH_4 production rates measured in laboratory incubations of sediment samples and seasonally averaged CH_4 ebullition rates estimated from high-frequency field observations has been reported for a shallow impounded river (Wilkinson et al. 2015), where $\sim$ 90% of the depth-integrated sediment potential CH_4 production rates were emitted to the atmosphere via ebullition. In other water bodies, the actual sediment CH_4 production rates can be considered to be lower than potential rates, due to the continuous, flow-dependent, supply of oxygen and alternative electron acceptors to the upper sediment from the overlying water (D'Ambrosio et al. 2022; Sun et al. 2022).

With potential CH_4 production rates measured in anaerobic laboratory incubations following a standardized protocol, we tested two main hypotheses: (1) sediment organic carbon content and depth below the sediment–water interface are universal drivers of depth-specific potential CH_4 production rates across aquatic systems. (2) Reservoirs have the highest potential CH_4 flux at the sediment–water interface due to generally higher sedimentation rates and organic carbon burial compared to rivers and lakes (Clow et al. 2015; Mendonça et al. 2017). We also hypothesize that the conversion efficiency of organic carbon to CH_4, which can be assessed through the molar ratio of potential production rates of CH_4 and CO_2, may differ between systems. Generally, we expect that potential CH_4 fluxes at the sediment–water interface constitute an upper limit or exceed the average emission rates at the air–water interface reported for the different types of aquatic systems in global assessments (Rosentreter et al. 2021).

Methods

Data sources and sediment incubations

The present study analyzed the most comprehensive dataset of potential CH_4 production rates in sediments from rivers, lakes, and reservoirs located in different climatic zones (Fig. 1). The data presented here are from two sources: (1) sediment incubations by the authors; (2) literature. In total, data on 238 sediment cores were collected in which 66 cores were prepared by the authors (unpublished). Sediment cores were collected using either a gravity corer (lakes and reservoirs) or a long cut-off syringe (rivers) (Supporting Information Table S1).

All potential CH_4 production rates were measured according to Saarnio et al. (1997). Duplicated sub-samples of 5–10 mL wet sediment (1187 samples in total) were extracted from different depth layers of each core (homogenized sediment samples from 2-cm-thick vertical slices). The sampling depths below the sediment–water interface were, for example, as follows: 1, 3, 5, 7, 9, 15, 25, and 40 cm with a smaller interval in the upper 10 cm and a greater interval at depths larger than 10 cm. The exact layer depths varied among datasets. The processing of the cores and samples was done in a nitrogen-flushed glove box with low-oxygen concentration to keep the samples under anaerobic conditions. The samples were transferred into nitrogen-flushed flasks (100 mL volume), which were sealed with butyl rubber stoppers and crimp capped. Hundred microliters of headspace gas samples was extracted regularly (weekly intervals) over 4–5 weeks and analyzed for CH_4 and CO_2 mixing ratios according to Wilkinson et al. (2018). Potential CH_4 production rates and potential CO_2 production rates were calculated from linear regressions of the increase in gas mixing ratios in the headspace over time (Fig. 1). Potential CH_4 production rates were normalized by the dry weight (DW) of the incubated sediment and reported in the unit $\mu g\ CH_4\ gDW^{-1}\ d^{-1}$.

Potential CH_4 production rates either reported in volumetric units or per sediment DW for 172 additional sediment cores could be gathered from the literature (Supporting Information Table S1, in total 238 cores and 66 unpublished were prepared by the authors). The literature data were selected based on strict screening criteria including comparable laboratory procedures. All data were categorized in the three system categories "Rivers," "Lakes," and "Reservoirs" (Fig. 1; Supporting Information Table S1). Given the large geographical gaps in our data (Fig. 1), with most sites sampled in the

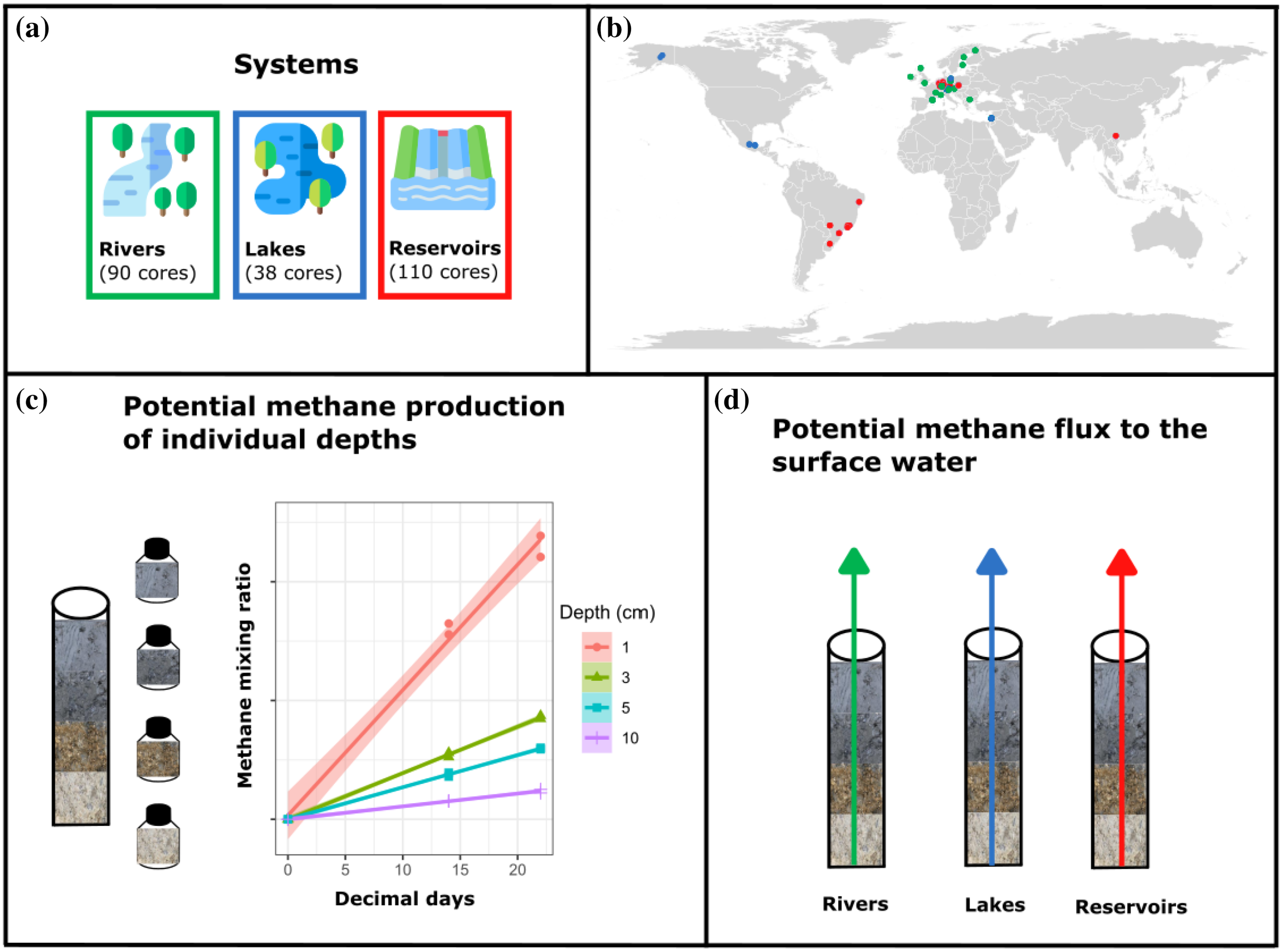

Fig. 1. Study design: The methane production potential of aquatic sediments was estimated from sediment cores that were collected from rivers, lakes, and reservoirs (**a**) located mainly in Europe with some representations from other continents (**b**). Subsamples from selected depths of individual cores were incubated under anaerobic conditions and at a constant temperature for 3–4 weeks in the laboratory. Methane (CH$_4$) and carbon dioxide production rates were estimated from the observed increase in headspace gas mixing ratios over time (**c**). The production rates measured in samples from different depths of the same core were vertically integrated to estimate the potential CH$_4$ flux across the sediment–water interface to the surface water (**d**).

northern hemisphere and data from "Rivers" were mostly obtained in Europe, global upscaling with these data is generally not recommended. With the distinct differences in sedimentation rates and sediment properties between rivers, lakes, and reservoirs, this study explores potential systematic differences, rather than analyzing the global significance of the three system categories.

For estimating depth-integrated potential production rates as a proxy of potential sediment-water fluxes (Fig. 1), we considered only data from incubations that reported the potential CH$_4$ production rate measurements for at least three slices from the upper 10 cm, not thicker than 3 cm each. Therefore, data with poor depth resolution were excluded from the depth-integrated analyses, resulting in 185 cores for core-based calculations: rivers ($n = 64$), lakes ($n = 20$), and reservoirs ($n = 66$).

Temperature adjustment

Since the sediment incubations compiled from the literature were conducted at different temperatures (T), we adjusted the measured potential production rates of CH$_4$ and CO$_2$ to those at a standard temperature of 20°C using the temperature coefficient theta (θ):

$$X_{20^\circ\mathrm{C}} = X_T 10^{\theta(20^\circ\mathrm{C}-T)} \tag{1}$$

We used a coefficient $\theta = 0.045^\circ\mathrm{C}^{-1}$, which was estimated by Wilkinson et al. (2019) for CH$_4$ production under anaerobic conditions in aquatic sediments.

In addition, Eq. (1) was used for adjusting measured production rates to the annual mean sediment temperature at each study site. For lakes and reservoirs, we assumed that the temperature of the upper sediment is approximately equal to the bottom water temperature. For rivers, the annual mean air temperature at the study sites was obtained from the nearest weather station (Czernecki et al. 2020). For most of the rivers, we estimated the annual mean water temperature from the annual mean air temperature, assuming equal temperatures of the upper sediments following Lauerwald et al. (2015). At the river "Wellbach" we got the water temperature from available monitoring data. For lakes and reservoirs, we retrieved either directly the annual mean sediment temperature or water temperatures at maximum depth from the site-related literature (Supporting Information Table S2).

Wet volume to DW conversion

Some studies provided data of potential production of CH_4 and CO_2 normalized by the volume of wet sediment (μg CH_4 mL^{-1} d^{-1}), whereas others were normalized by DW (μg CH_4 gDW^{-1} d^{-1}). In this study, we only use potential production rates per DW, and volumetric rates were converted using a conversion factor (C), which relates the sample volume (V_{WS}) to dry mass (m_{DW}):

$$V_{WS} = C \cdot m_{DW} \quad (2)$$

C was derived from sediment porosity (ε) and density of the solid sediment fraction ($\rho_S \approx 2.65\ 10^3$ kg m^{-3}):

$$C = \frac{1}{\rho_S(1-\varepsilon)} \quad (3)$$

Here we assumed that the sediment was water saturated, such that $V_W = \varepsilon V_{WS}$ and $V_S = (1-\varepsilon)V_{WS}$, with V_W and V_S denoting the volume of water and solid material in the sample, respectively. Depending on data availability, porosity was calculated either from the measured dry to wet mass ratio of the sample (R), from the water content in the sample (Z), or from wet bulk density (ρ_{WB}) as follows:

$$R = \frac{m_{DW}}{m_{WW}} = \frac{\rho_s(1-\varepsilon)}{\rho_s(1-\varepsilon)+\rho_w\varepsilon} \quad (4)$$

$$Z = \frac{m_W}{m_{WW}} = \frac{\rho_W\varepsilon}{\rho_S(1-\varepsilon)+\rho_w\varepsilon} \quad (5)$$

$$\rho_{WB} = \frac{m_{WW}}{V_{WS}} = \rho_S(1-\varepsilon)+\rho_w\varepsilon \quad (6)$$

with m_{WW} being the wet weight, m_w the mass of water, and ρ_W (10^3 kg m^{-3}) the density of water.

Depth integration

To determine the potential CH_4 flux at the sediment–water interface (F_{SWI} in mg CH_4 m^{-2} d^{-1}) for the individual cores, we calculated the cumulative areal CH_4 production rate of the sediment by numerical integration of potential CH_4 production rates (P in μg CH_4 gDW^{-1} d^{-1}) over the sampling depth (core length l) using the trapezoidal method:

$$F_{SWI} = C\int_0^l P(z)dz \quad (7)$$

For estimating the potential flux at in situ temperature ($F_{SWI\_in\ situ}$), we used Eq. (7) after adjusting the measured potential CH_4 production rates to the annual mean sediment temperature at each study site according to Eq. (1).

Organic carbon content

In the compiled datasets, sediment carbon content was determined using two different methods. For a set of 407 samples, the mass fraction of organic matter in the samples was measured as loss on ignition. For a second set of 633 samples, the mass fraction of organic carbon (OC) was measured using an elemental analyzer. Following Snowball and Sandgren (1996), a conversion factor of 2.0 was chosen to convert organic matter to organic carbon.

Statistics

Linear mixed-effect models were used to test: (i) the influence of the fixed effects sediment OC, sediment depth, sediment porosity, and climate zone on the response variable potential CH_4 production rates at different depths (four models: all systems, rivers, lakes, reservoirs), and (ii) the influence of the fixed variables core-averaged sediment OC, mean sediment porosity, climate zone, and latitude on the response variable F_{SWI_20} (at 20°C), as well as $F_{SWI\_in\ situ}$ (at mean annual sediment temperature) for all systems. For the models using data across all systems, we additionally tested system category (river, lake reservoir) as a fixed effect. We decided to exclude potential CO_2 production rates during the incubation from all models. Carbon dioxide production is intrinsically related to potential CH_4 production, and both of these parameters are measured in parallel. Koeppen-Geiger climate zones were added based on latitude and longitude with the "kgc" R-package (Bryant et al. 2017), which resulted in the following climate zones (abbreviations indicated in parentheses) covered by our dataset: tropical monsoon climate (Am), tropical wet and dry or savanna climate (Aw), hot semi-arid climate (BSh), humid subtropical climate (Cfa), temperate oceanic climate or subtropical highland climate (Cfb), hot-summer Mediterranean climate (Csa), monsoon-influenced humid subtropical climate (Cwa), subtropical highland climate or monsoon-influenced temperate oceanic climate (Cwb), warm-summer humid continental climate (Dfb), and subarctic climate (Dfc). We used the "lmer" function of the R-package "lme4" (Bates et al. 2015) with maximum likelihood estimation. For all linear mixed-effect models, we included system ID as a random effect on the intercept (22, 4, 4, and 14 levels for all systems, rivers, lakes, and reservoirs, respectively) to account for the fact that systems have a different number of samples. Linear mixed-effect models with system ID as a random effect performed better (i.e., had a lower Akaike information criterion value) compared to models with climate zone as a random effect. Statistical significance of fixed effects was assessed with likelihood ratio tests using the function "drop1" (Zuur et al. 2009). Co-correlated fixed effects, tested via the R-package "corrplot" (Pearson method) (Taiyun and Viliam 2021), were excluded if $r > 0.5$ (Zuur et al. 2009). The linear mixed-effect models were followed by model validations, checking the residuals for normal distribution and homogeneity of variances. Additionally, we checked that no climate zone was systematically underestimated or overestimated. For all linear mixed-effect models, we log-transformed the response variable to improve the model performance and validity, and z-scaled (i.e., standardized) the fixed effects to account for the different scales of each variable.

Differences in depth-specific molar ratios of produced CH_4 to CO_2, sediment OC content, potential CH_4 production rates, and $F_{\mathrm{SWI\_in\ situ}}$ across systems were tested with the Kruskal–Wallis and pairwise Wilcox methods. All statistics were performed in R (R Core Team 2023).

Results

Variability and drivers of potential CH_4 production rates

When standardized to a temperature of 20°C, the potential CH_4 production rates varied between zero (observed in sediment from rivers, lakes, and reservoirs) and a maximum value of 266.4 μg CH_4 gDW^{-1} d^{-1} (normalized to the DW of the incubated sample) in sediment from a temperate reservoir. While median values of potential CH_4 production rates were similar in river and lake sediments, the rates were a factor of five higher in reservoir sediments (Fig. 2a; Table 1). The potential production rates of CO_2 were slightly less variable, ranging from 0.04 in sediments from a temperate stream to 643.9 μg CO_2 gDW^{-1} d^{-1} in samples from a temperate reservoir. The molar ratio of CH_4 and CO_2 production rates had an overall median value close to unity (median 0.9 [Q1, Q3] [0.1, 1.4]), but the ratio was higher in reservoir sediment (1.1 [0.7, 1.5]) than in sediment from rivers (0.7 [0.1, 1.4]) and lakes (0.1 [0.04, 0.9]), respectively (Supporting Information Fig. S1). Potential CH_4 production rates were highest in the uppermost 10–20 cm of the sediments collected in rivers and lakes, whereas in reservoirs, the productive layer extended up to 60 cm depth below the sediment–water interface (Supporting Information Fig. S2). The analyzed sediment samples represented a wide range of porosity (16.1–98.2%) and OC content (0.4–24.5%). The OC content was < 10% in most samples; higher values were predominantly found in reservoir sediments. There were significant differences in OC content between different types of aquatic systems (Kruskal–Wallis; $p < 0.001$), with highest and lowest OC content in reservoir and river sediments, respectively. In sediment cores from lakes and reservoirs, the OC content declined with sediment depth, whereas the opposite trend was observed in river sediments (Supporting Information Fig. S3). Also, sediment porosity declined with sediment depth in lakes and reservoirs (Supporting Information Fig. S4).

Besides a strong positive correlation with potential production rates of CO_2 ($r = 0.89$, $r = 95$, and $r = 0.93$ for all systems combined, rivers, and reservoirs, respectively), there were no strong correlations ($r < 0.50$) between the individual explanatory parameters (OC, porosity, depth) and potential CH_4 production rates, except for OC in rivers ($r = 0.54$; Supporting Information Figs. S5, S6). Four different linear models (for data from all systems combined and for rivers, lakes, and reservoirs, respectively) showed significant effects of sediment OC content (positive) and depth (negative) on potential CH_4 production rates (Table 1). Porosity showed a significant positive effect for all systems and for lakes, while climate zone showed a significant effect on potential CH_4 production rates for all systems, lakes, and rivers (Table 1). Across all aquatic systems, system category (i.e., rivers, lakes, reservoirs) showed a significant effect on potential CH_4 production rates, and 60% of the variance in potential CH_4 production rates data was explained. In separate models for individual freshwater systems, the

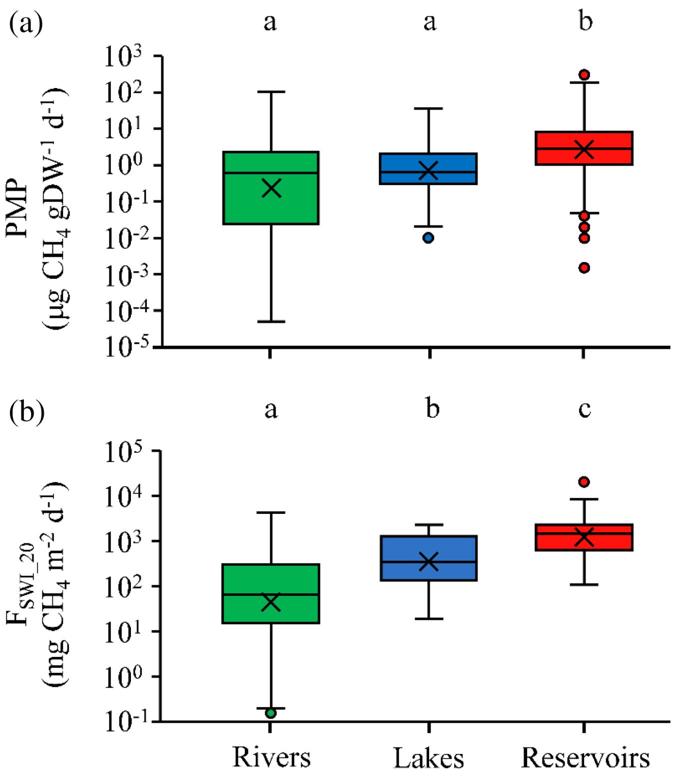

Fig. 2. (**a**) Potential methane production rates (PMP) in sediment samples from rivers, lakes, and reservoirs at standard temperature (20°C) and normalized by the dry weight (DW) of the sample. (**b**) Depth-integrated PMP for entire cores as an estimate of the potential CH_4 flux across sediment–water interface ($F_{\mathrm{SWI\_20}}$). In both panels, boxes stretch from the 1st to the 3rd quartiles, whiskers show the 1.5 * inter-quartile ranges, and values outside of this range are shown by circular symbols. The horizontal lines mark the median values, and the crosses show the mean values. Note the y-axes are log10-transformed. Significant differences between data from different aquatic systems are indicated by letters a, b, and c (Kruskal–Wallis and Post-hoc Wilcox test).

Table 1. Descriptive statistics and results of linear mixed models testing the fixed effects organic carbon content (OC), depth below the sediment–water interface (SWI), sediment porosity, and climate zone on the response variable potential CH_4 production rates (PMP) at a standard temperature of 20°C. System category (rivers, lakes, reservoirs) was additionally included as a fixed effect for the all-system model. Potential CO_2 production rate was not included in the models and only descriptive statistics are reported. System ID was included as a random effect on the intercept. The significance of fixed effects was assessed with likelihood ratio tests with degrees of freedom = 1. The direction (sign) of the effect is indicated with − or + when significant. Significant *p* values (< 0.05) are marked in bold. NA indicates variables that were either not suitable for individual models (system category) or variables that were excluded due to co-correlations.

	All systems[*] **($n = 934$)**	**Rivers**[†] **($n = 258$)**	**Lakes**[‡] **($n = 237$)**	**Reservoirs**[‖] **($n = 439$)**
	Q1, Q3	**Q1, Q3**	**Q1, Q3**	**Q1, Q3**
	Median	**Median**	**Median**	**Median**
	Mean ± SD	**Mean ± SD**	**Mean ± SD**	**Mean ± SD**
	χ^2 (1)	**χ^2 (1)**	**χ^2 (1)**	**χ^2 (1)**
	***p*-value (effect direction)**	***p*-value (effect direction)**	***p*-value (effect direction)**	***p*-value (effect direction)**
Response variable				
log10(PMP + 0.1) (μg CH_4 gDW^{-1} d^{-1})	0.4, 5.2	0.02, 3.0	0.3, 2.0	0.8, 8.7
	1.6	0.7	0.7	3.3
	6.8 ± 18.7	5.1 ± 14.7	1.7 ± 2.8	10.3 ± 23.7
Fixed effects				
OC (% of dry weight)	1.7, 5.9	0.5, 4.8	1.6, 2.9	3.1, 6.7
	3.4	1.6	2.1	4.9
	4.0 ± 3.1	2.8 ± 2.9	2.8 ± 2.1	5.3 ± 3.1
	88.79	109.66	19.30	41.32
	< **0.001** (+)	< **0.001** (+)	< **0.001** (+)	< **0.001** (+)
Depth (cm below SWI)	3.0, 25.8	3.0, 10.0	5.0, 56.8	3.5, 25.0
	9	5	21.0	10
	19.2 ± 24.5	11.4 ± 16.9	34.9 ± 35.4	16.7 ± 18.9
	71.46	31.89	31.93	50.81
	< **0.001** (−)	< **0.001** (−)	< **0.001** (−)	< **0.001** (−)
Porosity (−)	44.8, 78.1	42.2, 71.4	49.3, 71.4	45.9, 83.6
	61.9	55.3	58.9	70.2
	61.4 ± 19.5	56.5 ± 18.3	59.6 ± 15.9	65.5 ± 21.1
	58.95	NA	7.12	NA
	< **0.001** (+)		**0.008** (+)	
Climate zone	9.60	**7.90**	5.04	0.74
	0.048[§]	0.019[**]	0.025[††]	0.390
System category	5.90	NA	NA	NA
	0.052[‡‡]			
CO_2 production (μg CO_2 gDW^{-1} d^{-1})	2.9, 25.7	1.4, 9.6	6.3, 35.0	4.1, 24.1
	8.9	3.9	23.6	10.3
	21.2 ± 40.8	11.7 ± 27.0	22.6 ± 16.8	26.7 ± 53.9

[*] Marginal $R^2 = 0.393$, conditional $R^2 = 0.602$.

[†] Marginal $R^2 = 0.420$, conditional $R^2 = 0.494$.

[‡] Marginal $R^2 = 0.278$, conditional $R^2 = 0.348$.

[‖] Marginal $R^2 = 0.218$, conditional $R^2 = 0.572$.

[§] No significant pairwise differences.

[**] Cfb > Dfb ($p = 0.044$), Cfb = Dfc ($p = 0.280$), Dfb = Dfc ($p = 0.973$).

[††] No significant pairwise differences.

[‡‡] Reservoirs = lakes ($p = 0.092$), lakes = rivers ($p = 0.390$), reservoirs = rivers ($p = 0.803$).

models performed better for reservoir and river sediments (57% and 49% of the variance explained, respectively) than for lake sediment (35%; Table 1).

Potential CH_4 flux at the sediment–water interface

Vertical integration of the potential CH_4 production rates measured at standard temperature (20°C) in sediment cores provided estimates of the potential areal CH_4 flux across the sediment–water interface (F_{SWI_20}). The potential fluxes differed significantly between sediment cores from different aquatic systems (Kruskal–Wallis; $p < 0.001$) (Fig. 2b). The smallest median ([Q1, Q3]) flux (mg CH_4 m^{-2} d^{-1}) was found for river sediment (66.1 [16.2, 288.1]), in contrast to four times higher fluxes from lake sediment (242.5 [108.0, 792.0]), and more than 14 times higher fluxes from reservoir sediment (950.5 [465.0, 1473.9]).

The trends and correlations between the potential CH_4 fluxes and potential drivers mostly resemble those of the depth-specific potential CH_4 production rates (Fig. 3). A linear mixed model testing the effects of system category, sediment core-related mean OC and porosity, and climate zone on F_{SWI_20} combining all systems ($n = 147$) could explain 53% of the variance of the potential fluxes (Supporting Information Table S3). It was not tested for rivers ($n = 64$), lakes ($n = 20$), and reservoirs ($n = 66$) individually, because the limited number of samples per group does not support robust and reliable models. Mean OC content was the strongest predictor (positive), followed by climate zone, whereas mean porosity, indicating sediment physical characteristics, was not a significant explaining variable of F_{SWI_20}.

To account for the effect of sediment temperature under in situ conditions on the potential fluxes, we adjusted the specific potential CH_4 production rates (at 20°C) to the annual mean temperature at the sediment sampling sites before integration over depth ($F_{SWI\_in\ situ}$; Fig. 4, Table 2). We repeated the linear mixed model as for F_{SWI_20} (Supporting Information Table S4). System category, mean OC (positive), and climate zone were significant parameters, whereas mean porosity was not significant. 56% of the variance of $F_{SWI\_in\ situ}$ could be explained (Supporting Information Table S4).

A first comparison of available potential areal fluxes of CH_4 at the sediment–water interface ($F_{SWI\_in\ situ}$) showed consistently higher values than measured atmospheric emission rates from the different types of aquatic ecosystems that have been compiled in a recent meta-analysis (Fig. 4). The proportion of the emission rates at the water surface to $F_{SWI\_in\ situ}$ was highest in rivers (62.1%), followed by lakes (45.4%), and lowest in reservoirs (7.7%), if median values were used. When using mean values, the proportions were consistently higher, yet still lower in reservoirs than in lakes and in rivers (Table 2).

Discussion

Reservoir sediments are hotspots of CH_4 production

We found that reservoir sediments produce more CH_4 than sediments from rivers and lakes under standardized laboratory conditions. The differences were most pronounced in depth-integrated production rates, representing potential areal fluxes at the sediment–water interface (F_{SWI_20}), which were more than one order of magnitude higher in sediments from reservoirs compared to rivers (Fig. 2b). The large differences in potential areal fluxes among systems, compared to the smaller differences in potential CH_4 production rates measured in depth-specific sediment samples, suggest that the enhanced potential fluxes in reservoirs are supported by greater contributions (i.e., higher potential CH_4 production rates) from deeper sediment layers, where production rates were generally low in lakes and rivers (Supporting Information Fig. S2). Thus, the elevated CH_4 production potential of reservoir sediments is likely caused by the comparably high sedimentation rates

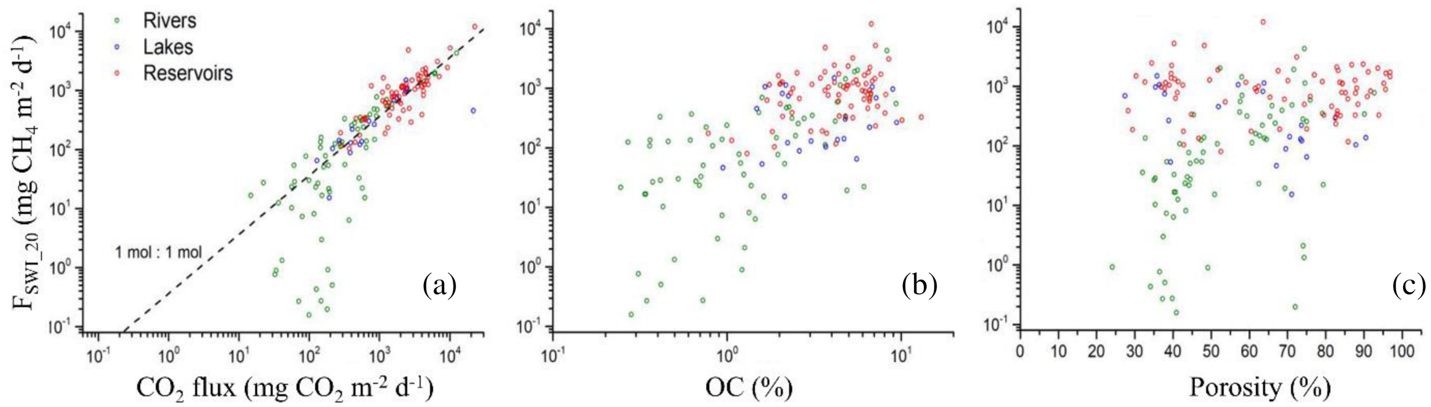

Fig. 3. Potential CH_4 fluxes across the sediment–water interface (SWI_20) in sediment cores from rivers (green symbols), lakes (blue symbols), and reservoirs (red symbols) vs. sediment properties: (**a**) vertically integrated potential CO_2 production rates (potential CO_2 flux), (**b**) mean (vertically averaged) organic carbon (OC) content, and (**c**) mean porosity. The potential CH_4 and CO_2 fluxes were corrected to a standard temperature of 20°C. The dashed line in (**a**) indicates a 1 : 1 relationship in molar units between the two fluxes.

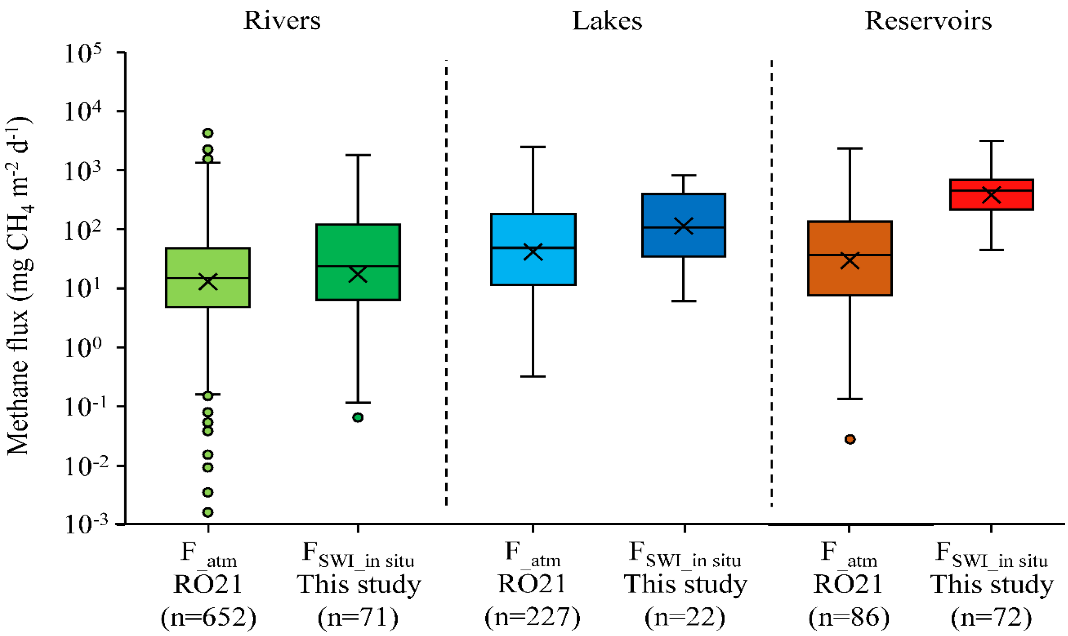

Fig. 4. Potential areal CH$_4$ flux across the sediment–water interface at in situ sediment temperature ($F_{\text{SWI\_in situ}}$) in rivers, lakes, and reservoirs, and atmospheric emissions rates compiled from globally distributed in situ flux (*F*_atm) by Rosentreter et al. (2021) (RO21). The boxplots show the medians of all stream sites (line), the first and third quartiles (hinges), the 1.5 * inter-quartile ranges (whiskers), and outliers outside the range of 1.5 * inter-quartile ranges (circular symbols). The sample number (*n*) is provided. The horizontal lines mark the median values, and the crosses show the mean values. Note the *y*-axis is log10-transformed.

and the associated supply of fresh organic matter (Berberich et al. 2020). In both shallow impounded rivers and larger reservoirs, higher CH$_4$ fluxes have often been reported in river inflow regions, where most terrestrial organic matter settles (DelSontro et al. 2011; Linkhorst et al. 2021; Sobek et al. 2012). In addition to sediment input, the properties of the flooded soil and the presence of terrestrial vegetation at the time of flooding have been found to affect CH$_4$ production in reservoir sediments (Abril et al. 2005; Rust et al. 2022). In contrast to the CH$_4$ production fueled by continuous sediment supply, however, these contributions decrease over time, resulting in a decline of CH$_4$ emissions with increasing reservoir age, as it has been found for some reservoirs (Barros et al. 2011).

Sediment OC content was a consistent control on depth-specific potential CH$_4$ production rates (Table 1; Supporting Information Figs. S5, S6). The uppermost, freshest sediment layers produced generally more CH$_4$ than deeper layers, and sediment depth was also an important predictor for potential CH$_4$ production rates across systems (Table 1). In sediment incubation studies for which the age of the sediment was estimated, it was found that the youngest sediment layers (< 6–12 yr old in tropical reservoirs and 30–150 yr in Northern lakes) contribute most to the depth-integrated CH$_4$ production (Isidorova et al. 2019; Moras et al. 2024). These studies further found that age and total nitrogen were the best predictors of potential CH$_4$ production rates. Total nitrogen content of the sediment was suggested as a proxy for OC reactivity of the sediment and thus a better predictor for potential CH$_4$ production rates than OC (Moras et al. 2024). Because estimates of sediment age were not available, we could not test to what extent the empirical relationship suggested by these authors (Moras et al. 2024) would also hold for the larger dataset analyzed here. Nevertheless, the mechanistic models often assume an exponential decline of potential CH$_4$ production rates with increasing sediment depth (Langenegger et al. 2019; Sabrekov et al. 2017), which has also been described for individual cores of the dataset analyzed here (Wilkinson et al. 2019). However, no consistent depth dependence has been found in other sediment cores (Bodmer et al. 2020; Liu, Sotiri, et al. 2020; Liu, Yang, et al. 2020). In this study, we identified sediment depth as a universal driver beyond individual studies but acknowledge that the variability of potential CH$_4$ production rates related to depth within and among systems remains high (Supporting Information Fig. S5). More accurate empirical predictions require additional site-specific parameters, including sedimentation rate or sediment age, and additional measures of the quality of sediment OM, including nitrogen (Moras et al. 2024).

The high production potential of reservoir sediments was associated with a higher molar ratio of produced CH$_4$ to CO$_2$ (Supporting Information Fig. S1). The median ratio of 1.1 observed in reservoir sediments is close to the expected 1 : 1 ratio for the complete fermentation of glucose to methanogenesis. For stoichiometric reasons, one-third of the total CH$_4$ is produced by hydrogenotrophic methanogenesis, using hydrogen derived from

Table 2. Potential areal CH_4 flux across the sediment–water interface adjusted to the site-specific mean annual sediment temperature ($F_{SWI\_in\ situ}$), atmospheric emission rates (F_atm), and the proportion of emission to production ($F\_atm/F_{SWI\_in\ situ} * 100$) for different types of aquatic systems. Statistics on global atmospheric emission rates from aquatic systems were adopted from a recent meta-analysis of flux measurements (Rosentreter et al. 2021).

	Rivers				Lakes				Reservoirs			
	n	Median	Q1, Q3	Mean ± SD	*n*	Median	Q1, Q3	Mean ± SD	*n*	Median	Q1, Q3	Mean ± SD
$F_{SWI\_in\ situ}$ (mg CH_4 m^{-2} d^{-1})	71	24.0	6.4, 106.8	111.8 ± 265.9	22	106.9	35.3, 363.7	234.9 ± 253.5	72	450.6	220.9, 677.5	548.3 ± 533.9
F_atm (mg CH_4 m^{-2} d^{-1})	652	14.9	4.3, 47.0	113 ± 426	227	48.5	11.8, 177.4	153 ± 294	86	34.7	6.6, 124.2	161 ± 368
Proportion (%)		62.1		101.1		45.4		65.1		7.7		29.4

the initial fermentation, while the remaining two-thirds originate from the acetate via acetoclastic methanogenesis (Conrad 1999, 2020). A recent meta-analysis of microcosm incubations of sediments and water-logged soils, however, revealed that such high ratios are rarely observed (Zhu et al. 2023). The median value of 0.1 reported in that study closely aligns with the value we observed in lake sediments. Zhu et al. (2023) further demonstrated that the ratio remains below one whenever hydrogen or acetate escapes, or gets used in a non-methanogenic pathway. The significant differences in CH_4-to-CO_2 production ratios across aquatic systems therefore suggest variations in biogeochemical cycling as a potential driver of the elevated CH_4 production in reservoir sediments. To identify the underlying mechanisms, future measurements of potential CH_4 production rates should include the characterization of the isotopic composition of both gases, which would help constrain methanogenic pathways (Berberich et al. 2020; Gruca-Rokosz et al. 2020).

Previous studies identified the productivity of the aquatic system and trophic state as important predictors for sediment CH_4 production (Moras et al. 2024; West et al. 2016). Compared to terrestrial-derived OC, phytoplankton addition results in a more rapid production of CH_4 within some days to weeks after addition (Grasset et al. 2018; West et al. 2012). Although we cannot evaluate the effect of eutrophication due to the lack of information about trophic state for most of our data, there is increasing evidence from the literature, particularly for lakes and reservoirs.

Potential areal CH_4 production exceeds atmospheric emissions

The depth-integrated potential areal CH_4 fluxes at the sediment–water interface ($F_{SWI\_in\ situ}$) in rivers, lakes, and reservoirs are consistently higher than atmospheric emission rates from these systems, as they were recently compiled from globally distributed flux measurements (Rosentreter et al. 2021) (Fig. 4). When considering median values, the CH_4 emissions to the atmosphere represent 62% of the potential fluxes at the sediment–water interface in rivers, followed by lakes (45%) and reservoirs (8%). The differences in the proportion of emission to production between the different types of aquatic systems, however, change when considering mean values instead of medians, due to the highly skewed distributions of the fluxes (Table 2). Overall, the comparison suggests that observed atmospheric emission rates represent 8–62% of the sediment potential CH_4 production rates. Given the limited and geographically biased distribution of measured potential production rates and the different spatial and temporal scales over which sediment production and atmospheric emission rates were estimated, this comparison needs to be interpreted with caution, and more comprehensive data on potential CH_4 production rates and longer-term averaged atmospheric emission estimates for the same water body are required for constraining these first estimates. Moreover, the depth integrated fluxes at mean ecosystem temperature appear more similar between reservoirs and rivers (Table 2). This temperature sensitivity underscores the importance of being able to map reservoir and lake bathymetry (and associated bottom temperatures) better for informing large-scale estimates.

The difference between $F_{\mathrm{SWI\_in\ situ}}$ and atmospheric emission rates can generally be attributed to the reduction of CH$_4$ production under in-situ conditions and by aerobic CH$_4$ oxidation at the SWI and in the water column. Moreover, the potential CH$_4$ production rates estimated from anaerobic sediment incubations can be expected to overestimate the net in situ rates, where not all parts of the sediment cores are oxygen-depleted. The oxygen penetration depth into sediment is typically limited by mass transfer across the SWI. In fast-flowing streams with coarser sediment, oxygen transport can be enhanced by advective flows and can reach several centimeters to decimeters (Galloway et al. 2019; Kaufman et al. 2017). Thus, the relatively short sediment cores sampled from rivers (mostly $\sim$ 10 cm) may not be representative for in situ production rates in these systems. In slow-flowing environments, such as lakes and reservoirs, oxygen penetration is often limited to some millimeters or less (Lorke et al. 2003) and the CH$_4$ production estimated under laboratory conditions might be closer to in situ rates. Under these conditions, the upward flux of CH$_4$ is reduced by aerobic CH$_4$ oxidation in the top sediment layer and in the water column. In accordance with the average ratio of emission rates to sediment potential CH$_4$ production rates (Table 2), estimates of ecosystem CH$_4$ oxidation suggest that between 30% and 90% of the produced CH$_4$ can be oxidized (Lei et al. 2019; Sawakuchi et al. 2016), yet a systematic analysis of oxidation rates across different aquatic systems is currently lacking. However, many existing estimates of CH$_4$ emissions and ecosystem oxidation rates have neglected bubble-mediated fluxes, which can be the main emission pathway and efficiently bypass oxidation in shallow aquatic systems. Under these conditions, the atmospheric emission rates can closely correspond to sediment potential CH$_4$ production rates, as it has been found in a temperate run-off-river reservoir (Wilkinson et al. 2015).

Our estimates of $F_{\mathrm{SWI\_in\ situ}}$ strongly exceed the fluxes at the SWI that have been obtained in a recent meta-analysis of measurements from lakes (D'Ambrosio and Harrison 2021), where mean and median CH$_4$ fluxes were a factor of 26 and 140 lower than $F_{\mathrm{SWI\_in\ situ}}$ from lake sediment (*see* Supporting Information Fig. S7 for a comparison of flux estimates from both studies). In contrast to the potential fluxes estimated using a standardized incubation method and incubation conditions, the fluxes reported in the former study were compiled from data obtained under different incubation conditions. While it is expected that the potential CH$_4$ production rates-based sediment-water fluxes exceed those under in-situ conditions, the large magnitude of the differences is rather surprising. It should be noted, however, that the CH$_4$ fluxes reported by D'Ambrosio and Harrison (2021) are also substantially lower than the reported atmospheric emission rates from lakes (Rosentreter et al. 2021). These contrasting findings underscore the need for an improved understanding of CH$_4$ production and consumption pathways in aquatic ecosystems.

Implications

The first meta-analysis of potential CH$_4$ production rates in sediments from different types of freshwater aquatic systems presented in this study improves our process understanding of quantitative inland-water CH$_4$ budgets. Existing larger-scale assessments of inland–water CH$_4$ emissions are based on upscaling of mostly sparse and episodic flux measurements. The accuracy of these estimates and, more importantly, the ability to predict their responses and feedback to ongoing and future environmental changes require mechanistic understanding of the processes that regulate CH$_4$ dynamics in different types of inland waters. Such models have recently been developed for rivers (McGinnis et al. 2016), lakes (Stepanenko et al. 2016; Zhuang et al. 2023), and reservoirs (Delwiche et al. 2022), and require knowledge on CH$_4$ fluxes across the SWI, or on the vertical distribution of CH$_4$ production rates in sediment. The potential CH$_4$ production rates obtained under standardized conditions provide important constraints on the magnitude and variability of sediment CH$_4$ production and reveal consistent differences between aquatic systems. The quantitative description of sediment potential CH$_4$ production rates in terms of potentially relevant drivers, as it is required for a perspective integration of inland waters in land surface and earth system models, revealed OC content and depth as universal drivers across systems and sediment porosity as a more system-specific driver. In wetland biogeochemical models, sediment CH$_4$ production rates were either estimated from degradation of different pools of organic matter (Wania et al. 2010), or additionally considering the kinematics of organic matter decomposition, the precursors (acetate and hydrogen) and alternative electron acceptors (Ricciuto et al. 2021). The distinct anaerobic degradation kinetics of different types of autochthonous and allochthonous organic matter to CH$_4$ in aquatic sediments (Grasset et al. 2021; West et al. 2012) suggest that such approaches could also be applied for estimating depth profiles of potential CH$_4$ production rates in aquatic sediments based on known deposition rates and organic matter composition.

The observed shift in the conversion efficiency of OC in favor of CH$_4$ vs. CO$_2$ in reservoir sediment has important implications for the longer-term assessment of aquatic CH$_4$ emissions. Higher OC burial rates have been reported for reservoirs in comparison to rivers and lakes because of the high sediment trapping efficiency and reduced oxygen exposure time in reservoirs (Clow et al. 2015; Mendonça et al. 2017). This supports our discussion on sedimentation rates as the main reason for higher CH$_4$ production in reservoir sediments compared to sediments from rivers and lakes under standardized laboratory conditions. As the original carbon source of organic material that fuels CH$_4$ production in inland waters is atmospheric CO$_2$, the CH$_4$ emissions are ultimately associated with a conversion of atmospheric CO_2 to CH_4, and with an around 30-fold increase of its contribution to the current radiative forcing on a 100-yr timescale (Etminan et al. 2016). The disproportional high CH_4 production rate in sediments from human-made water bodies calls for more comprehensive monitoring of their CH_4 emissions and their consideration in the assessment of carbon footprints of reservoirs (Harrison et al. 2021) as well as for reservoir management practices (e.g., Lessmann et al. 2023). Sedimentation, which appears to be the main driver of potential CH_4 production, also decreases the storage volume of reservoirs and therewith reduces their economic and societal values (Wisser et al. 2013). Efforts to address these challenges by improved sediment management should consider CH_4 emissions as an additional drawback of sediment retention.

Author Contributions

Pascal Bodmer, Christoph Bors, Liu Liu, and Andreas Lorke conceived the study design. Pascal Bodmer and Christoph Bors compiled, processed, analyzed, and visualized the data. Christoph Bors, Pascal Bodmer, and Liu Liu compiled the literature data for the mean annual sediment temperatures. Pascal Bodmer, Liu Liu, and Andreas Lorke co-wrote the paper with input from Christoph Bors.

Acknowledgments

We would like to thank Lediane Marcon, Florian Burgis, and Jeremy Wilkinson for contributing data and Vincent Fugère for his helpful input related to the linear mixed models. This study was financially supported by the German Research Foundation (Grants LO 1150/5-2, LO 1150/14-1, BO 5050/1-1) and the National Natural Science Foundation of China (Grant No. 42207089, 42311530334), the Yunnan Natural Science Foundation Project (202401AT070132), the Yunnan Provincial Science and Technology Project at Southwest United Graduate School (202302AP370001), and the Yunnan Provincial Major Science and Technology Special Project (202203AC100002). We thank the reviewers for their constructive feedback, which improved the manuscript.

Conflicts of Interest

None declared.

References

Abril, G., F. Guérin, S. Richard, et al. 2005. "Carbon Dioxide and Methane Emissions and the Carbon Budget of a 10-Year Old Tropical Reservoir (Petit Saut, French Guiana)." *Global Biogeochemical Cycles* 19: GB4007. https://doi.org/10.1029/2005GB002457.

Barros, N., J. J. Cole, L. J. Tranvik, et al. 2011. "Carbon Emission From Hydroelectric Reservoirs Linked to Reservoir Age and Latitude." *Nature Geoscience* 4: 593–596. https://doi.org/10.1038/ngeo1211.

Bastviken, D. 2009. "Methane." In Encyclopedia of Inland Waters, edited by G. E. Likens, vol. 2. Oxford: Elsevier. https://doi.org/10.1016/B978-012370626-3.00117-4.

Bastviken, D., J. J. Cole, M. L. Pace, and M. C. Van de Bogert. 2008. "Fates of Methane From Different Lake Habitats: Connecting Whole-Lake Budgets and CH_4 Emissions." *Journal of Geophysical Research – Biogeosciences* 113: G02024. https://doi.org/10.1029/2007JG000608.

Bastviken, D., L. J. Tranvik, J. A. Downing, P. M. Crill, and A. Enrich-Prast. 2011. "Freshwater Methane Emissions Offset the Continental Carbon Sink." *Science* 331: 50. https://doi.org/10.1126/science.119680.

Bates, D., M. Mächler, B. Bolker, and S. Walker. 2015. "Fitting Linear Mixed-Effects Models Using lme4." *Journal of Statistical Software* 67: 1–48. https://doi.org/10.18637/jss.v067.i01.

Berberich, M. E., J. J. Beaulieu, T. L. Hamilton, S. Waldo, and I. Buffam. 2020. "Spatial Variability of Sediment Methane Production and Methanogen Communities Within a Eutrophic Reservoir: Importance of Organic Matter Source and Quantity." *Limnology and Oceanography* 65: 1336–1358. https://doi.org/10.1002/lno.11392.

Bodmer, P., R. J. E. Vroom, T. Stepina, P. A. del Giorgio, and S. Kosten. 2024. "Methane Dynamics in Vegetated Habitats in Inland Waters: Quantification, Regulation, and Global Significance." *Frontiers in Water* 5: 1332968. https://doi.org/10.3389/frwa.2023.1332968.

Bodmer, P., J. Wilkinson, and A. Lorke. 2020. "Sediment Properties Drive Spatial Variability of Potential Methane Production and Oxidation in Small Streams." *Journal of Geophysical Research – Biogeosciences* 125, no. 1: e2019JG005213. https://doi.org/10.1029/2019JG005213.

Bogard, M., P. del Giorgio, L. Boutet, et al. 2014. "Oxic Water Column Methanogenesis as a Major Component of Aquatic CH_4 Fluxes." *Nature Communications* 5: 5350. https://doi.org/10.1038/ncomms6350.

Bryant, C., N. Wheeler, F. Rubel, and R. French. 2017. Kgc: Koeppen-Geiger climatic zones R Package Version 1.0.0.2. https://doi.org/10.32614/CRAN.package.kgc.

Clow, D. W., S. M. Stackpoole, K. L. Verdin, D. E. Butman, and R. G. Striegl. 2015. "Organic Carbon Burial in Lakes and Reservoirs of the Conterminous United States." *Environmental Science & Technology* 49: 7614–7622. https://doi.org/10.1021/acs.est.5b00373.

Conrad, R. 1999. "Contribution of Hydrogen to Methane Production and Control of Hydrogen Concentrations in Methanogenic Soils and Sediments." *FEMS Microbiology Ecology* 28: 193–202. https://doi.org/10.1111/j.1574-6941.1999.tb00575.x.

Conrad, R. 2020. "Importance of Hydrogenotrophic, Aceticlastic and Methylotrophic Methanogenesis for Methane Production in Terrestrial, Aquatic and Other Anoxic Environments: A Mini Review." *Pedosphere* 30: 25–39. https://doi.org/10.1016/S1002-0160(18)60052-9.

Czernecki, B., A. Głogowski, and J. Nowosad. 2020. "Climate: An R Package to Access Free In-Situ Meteorological and Hydrological Datasets for Environmental Assessment." *Sustainability* 12: 394. https://doi.org/10.3390/su12010394.

D'Ambrosio, S. L., and J. A. Harrison. 2021. "Methanogenesis Exceeds CH$_4$ Consumption in Eutrophic Lake Sediments." *Limnology and Oceanography Letters* 6: 173–181. https://doi.org/10.1002/lol2.10192.

D'Ambrosio, S. L., S. M. Henderson, J. R. Nielson, and J. A. Harrison. 2022. "In Situ Flux Estimates Reveal Large Variations in Methane Flux Across the Bottom Boundary Layer of a Eutrophic Lake." *Limnology and Oceanography* 67: 2119–2139. https://doi.org/10.1002/lno.12193.

Deemer, B., and M. A. Holgerson. 2021. "Drivers of Methane Flux Differ Between Lakes and Reservoirs, Complicating Global Upscaling Efforts." *Journal of Geophysical Research – Biogeosciences* 126: e2019JG005600. https://doi.org/10.1029/2019JG005600.

Deemer, B. R., J. A. Harrison, S. Li, et al. 2016. "Greenhouse Gas Emissions From Reservoir Water Surfaces: A New Global Synthesis." *Bioscience* 66: 949–964. https://doi.org/10.1093/biosci/biw117.

DelSontro, T., M. J. Kunz, T. Kempter, A. Wüest, B. Wehrli, and D. B. Senn. 2011. "Spatial Heterogeneity of Methane Ebullition in a Large Tropical Reservoir." *Environmental Science & Technology* 45: 9866–9873. https://doi.org/10.1021/es2005545.

Delwiche, K. B., J. A. Harrison, J. D. Maasakkers, et al. 2022. "Estimating Drivers and Pathways for Hydroelectric Reservoir Methane Emissions Using a New Mechanistic Model." *Journal of Geophysical Research – Biogeosciences* 127: e2022JG006908. https://doi.org/10.1029/2022JG006908.

Encinas Fernández, J., F. Peeters, and H. Hofmann. 2016. "On the Methane Paradox: Transport From Shallow Water Zones Rather than In Situ Methanogenesis Is the Major Source of CH$_4$ in the Open Surface Water of Lakes." *Journal of Geophysical Research – Biogeosciences* 121: 2717–2726. https://doi.org/10.1002/2016JG003586.

Etminan, M., G. Myhre, E. J. Highwood, and K. P. Shine. 2016. "Radiative Forcing of Carbon Dioxide, Methane, and Nitrous Oxide: A Significant Revision of the Methane Radiative Forcing." *Geophysical Research Letters* 43: 12614–12623. https://doi.org/10.1002/2016GL071930.

Galloway, J., A. Fox, J. Lewandowski, and S. Arnon. 2019. "The Effect of Unsteady Streamflow and Stream-Groundwater Interactions on Oxygen Consumption in a Sandy Streambed." *Scientific Reports* 9: 19735. https://doi.org/10.1038/s41598-019-56289-y.

Grasset, C., R. Mendonça, G. Villamor Saucedo, D. Bastviken, F. Roland, and S. Sobek. 2018. "Large But Variable Methane Production in Anoxic Freshwater Sediment Upon Addition of Allochthonous and Autochthonous Organic Matter." *Limnology and Oceanography* 63: 1488–1501. https://doi.org/10.1002/lno.10786.

Grasset, C., S. Moras, A. Isidorova, R.-M. Couture, A. Linkhorst, and S. Sobek. 2021. "An Empirical Model to Predict Methane Production in Inland Water Sediment From Particular Organic Matter Supply and Reactivity." *Limnology and Oceanography* 66: 3643–3655. https://doi.org/10.1002/lno.11905.

Gruca-Rokosz, R., D. Szal, L. Bartoszek, and A. Pękala. 2020. "Isotopic Evidence for Vertical Diversification of Methane Production Pathways in Freshwater Sediments of Nielisz Reservoir (Poland)." *Catena* 195: 104803. https://doi.org/10.1016/j.catena.2020.104803.

Harrison, J. A., Y. T. Prairie, S. Mercier-Blais, and C. Soued. 2021. "Year-2020 Global Distribution and Pathways of Reservoir Methane and Carbon Dioxide Emissions According to the Greenhouse Gas From Reservoirs (G-Res) Model." *Global Biogeochemical Cycles* 35: e2020GB006888. https://doi.org/10.1029/2020GB006888.

Isidorova, A., C. Grasset, R. Mendonça, and S. Sobek. 2019. "Methane Formation in Tropical Reservoirs Predicted From Sediment Age and Nitrogen." *Scientific Reports* 9: 11017. https://doi.org/10.1038/s41598-019-47346-7.

Jansen, J., B. F. Thornton, A. Cortés, et al. 2020. "Drivers of Diffusive CH$_4$ Emissions From Shallow Subarctic Lakes on Daily to Multi-Year Timescales." *Biogeosciences* 17: 1911–1932. https://doi.org/10.5194/bg-17-1911-2020.

Kaufman, M. H., M. B. Cardenas, J. Buttles, A. J. Kessler, and P. L. M. Cook. 2017. "Hyporheic Hot Moments: Dissolved Oxygen Dynamics in the Hyporheic Zone in Response to Surface Flow Perturbations." *Water Resources Research* 53: 6642–6662. https://doi.org/10.1002/2016WR020296.

Langenegger, T., D. Vachon, D. Donis, and D. McGinnis. 2019. "What the Bubble Knows: Lake Methane Dynamics Revealed by Sediment Gas Bubble Composition." *Limnology and Oceanography* 64: 1526–1544. https://doi.org/10.1002/lno.11133.

Lauerwald, R., G. G. Laruelle, J. Hartmann, P. Ciais, and P. A. Regnier. 2015. "Spatial Patterns in CO$_2$ Evasion From the Global River Network." *Global Biogeochemical Cycles* 29: 534–554. https://doi.org/10.1002/2014GB004941.

Lei, D., J. Liu, J. Zhang, et al. 2019. "Methane Oxidation in the Water Column of Xiangxi Bay, Three Gorges Reservoir." *CLEAN - Soil, Air, Water* 47: 1800516. https://doi.org/10.1002/clen.201800516.

Lessmann, O., J. Encinas Fernández, K. Martínez-Cruz, and F. Peeters. 2023. "Methane Emissions Due to Reservoir Flushing: A Significant Emission Pathway?" *Biogeosciences* 20: 4057–4068. https://doi.org/10.5194/bg-20-4057-2023.

Linkhorst, A., J. R. Paranaíba, R. Mendonça, et al. 2021. "Spatially Resolved Measurements in Tropical Reservoirs Reveal Elevated Methane Ebullition at River Inflows and at High Productivity." *Global Biogeochem. Cy.* 35: e2020GB006717. https://doi.org/10.1029/2020GB006717.

Liu, L., K. Sotiri, Y. Dück, et al. 2020. "The Control of Sediment Gas Accumulation on Spatial Distribution of Ebullition in Lake Kinneret." *Geo-Marine Letters* 40: 453–466. https://doi.org/10.1007/s00367-019-00612-z.

Liu, L., J. Wilkinson, K. Koca, C. Buchmann, and A. Lorke. 2016. "The Role of Sediment Structure in Gas Bubble Storage and Release." *Journal of Geophysical Research – Biogeosciences* 121: 1992–2005. https://doi.org/10.1002/2016JG003456.

Liu, L., Z. Yang, K. Delwiche, et al. 2020. "Spatial and Temporal Variability of Methane Emissions From Cascading Reservoirs in the Upper Mekong River." *Water Research* 186: 116319. https://doi.org/10.1016/j.watres.2020.116319.

Liu, L., X. Zhang, S. Schorn, et al. 2024. "Strong Subseasonal Variability of Oxic Methane Production Challenges Methane Budgeting in Freshwater Lakes." *Environmental Science & Technology* 58: 19690–19701. https://doi.org/10.1021/acs.est.4c07413.

Lorke, A., B. Müller, M. Maerki, and A. Wüest. 2003. "Breathing Sediments: The Control of Diffusive Transport across the Sediment–Water Interface by Periodic Boundary-Layer Turbulence." *Limnology and Oceanography* 48: 2077–2085. https://doi.org/10.4319/lo.2003.48.6.2077.

MacIntyre, S., R. Wanninkhof, and J. Chanton. 1995. "Trace Gas Exchange across the Airwater Interface in Freshwater and Coastal Marine Environments." In Measuring Emissions From Soil and Water, edited by P. A. Matson and R. C. Harriss. Cambridge: Blackwell Science Ltd.

Maeck, A., H. Hofmann, and A. Lorke. 2014. "Pumping Methane out of Aquatic Sediments–Ebullition Forcing Mechanisms in an Impounded River." *Biogeosciences* 11: 2925–2938. https://doi.org/10.5194/bg-11-2925-2014.

Mayr, M. J., M. Zimmermann, J. Dey, A. Brand, B. Wehrli, and H. Bürgmann. 2020. "Growth and Rapid Succession of Methanotrophs Effectively Limit Methane Release during Lake Overturn." *Communications Biology* 3: 108. https://doi.org/10.1038/s42003-020-0838-z.

McGinnis, D. F., N. Bilsley, M. Schmidt, et al. 2016. "Deconstructing Methane Emissions From a Small Northern-European River: Hydrodynamics and Temperature as Key Drivers." *Environmental Science & Technology* 50: 11680–11687. https://doi.org/10.1021/acs.est.6b03268.

McGinnis, D. F., J. Greinert, Y. Artemov, S. Beaubien, and A. Wüest. 2006. "Fate of Rising Methane Bubbles in Stratified Waters: How Much Methane Reaches the Atmosphere?" *Journal of Geophysical Research: Oceans* 111: C09007. https://doi.org/10.1029/2005JC003183.

Mendonça, R., R. A. Müller, D. Clow, et al. 2017. "Organic Carbon Burial in Global Lakes and Reservoirs." *Nature Communications* 8: 1694. https://doi.org/10.1038/s41467-017-01789-6.

Moras, S., U. R. Zellmer, E. Hiltunen, C. Grasset, and S. Sobek. 2024. "Predicting Methane Formation Rates of Freshwater Sediments in Different Biogeographic Regions." *Journal of Geophysical Research – Biogeosciences* 129: 2023JG007463. https://doi.org/10.1029/2023JG007463.

R Core Team, R. 2023. R: A language and environment for statistical computing.

Reed, D. C., B. R. Deemer, S. van Grinsven, and J. A. Harrison. 2017. "Are Elusive Anaerobic Pathways Key Methane Sinks in Eutrophic Lakes and Reservoirs?" *Biogeochemistry* 134: 29–39. https://doi.org/10.1007/s10533-017-0356-3.

Ricciuto, D. M., X. Xu, X. Shi, et al. 2021. "An Integrative Model for Soil Biogeochemistry and Methane Processes: I. Model Structure and Sensitivity Analysis." *Journal of Geophysical Research – Biogeosciences* 126: e2019JG005468. https://doi.org/10.1029/2020JG005963.

Rosentreter, J. A., A. V. Borges, B. R. Deemer, et al. 2021. "Half of Global Methane Emissions Come From Highly Variable Aquatic Ecosystem Sources." *Nature Geoscience* 14: 225–230. https://doi.org/10.1038/s41561-021-00715-2.

Rust, F., P. Bodmer, and P. Del Giorgio. 2022. "Modeling the Spatial and Temporal Variability in Surface Water CO_2 and CH_4 Concentrations in a Newly Created Complex of Boreal Hydroelectric Reservoirs." *Science of the Total Environment* 815: 152459. https://doi.org/10.1016/j.scitotenv.2021.152459.

Saarnio, S., J. Alm, J. Silvola, A. Lohila, H. Nykänen, and P. J. Martikainen. 1997. "Seasonal Variation in CH_4 Emissions and Production and Oxidation Potentials at Microsites on an Oligotrophic Pine Fen." *Oecologia* 110: 414–422. https://doi.org/10.1007/s004420050176.

Sabrekov, A. F., B. R. Runkle, M. V. Glagolev, et al. 2017. "Variability in Methane Emissions From West Siberia's Shallow Boreal Lakes on a Regional Scale and its Environmental Controls." *Biogeosciences* 14: 3715–3742. https://doi.org/10.5194/bg-14-3715-2017.

Saunois, M., A. R. Stavert, B. Poulter, et al. 2020. "The Global Methane Budget 2000–2017." *Earth System Science Data* 12: 1561–1623. https://doi.org/10.5194/essd-12-1561-2020.

Sawakuchi, H. O., D. Bastviken, A. O. Sawakuchi, et al. 2016. "Oxidative Mitigation of Aquatic Methane Emissions in Large Amazonian Rivers." *Global Change Biology* 22: 1075–1085. https://doi.org/10.1111/gcb.13169.

Segers, R. 1998. "Methane Production and Methane Consumption: A Review of Processes Underlying Wetland Methane Fluxes." *Biogeochemistry* 41: 23–51. https://doi.org/10.1023/A:1005929032764.

Snowball, I., and P. Sandgren. 1996. "Lake Sediment Studies of Holocene Glacial Activity in the Kårsa Valley, Northern Sweden: Contrasts in Interpretation." *Holocene* 6: 367–372. https://doi.org/10.1177/0959683696006003.

Sobek, S., T. DelSontro, N. Wongfun, and B. Wehrli. 2012. "Extreme Organic Carbon Burial Fuels Intense Methane Bubbling in a Temperate Reservoir." *Geophysical Research Letters* 39: L01401. https://doi.org/10.1029/2011GL050144.

Stanley, E. H., N. J. Casson, S. T. Christel, J. T. Crawford, L. C. Loken, and S. K. Oliver. 2016. "The Ecology of Methane in Streams and Rivers: Patterns, Controls, and Global Significance." *Ecological Monographs* 86: 146–171. https://doi.org/10.1890/15-1027.

Stepanenko, V., I. Mammarella, A. Ojala, H. Miettinen, V. Lykosov, and T. Vesala. 2016. "LAKE 2.0: A Model for Temperature, Methane, Carbon Dioxide and Oxygen Dynamics in Lakes." *Geoscientific Model Development* 9: 1977–2006. https://doi.org/10.5194/gmd-9-1977-2016.

Sun, H., R. Yu, X. Liu, et al. 2022. "Drivers of Spatial and Seasonal Variations of CO_2 and CH_4 Fluxes at the Sediment Water Interface in a Shallow Eutrophic Lake." *Water Research* 222: 118916. https://doi.org/10.1016/j.watres.2022.118916.

Taiyun, W., and S. Viliam. 2021. "R Package 'Corrplot': Visualization of a Correlation Matrix (Version 0.92)." https://github.com/taiyun/corrplot.

Wania, R., I. Ross, and I. Prentice. 2010. "Implementation and Evaluation of a New Methane Model Within a Dynamic Global Vegetation Model: LPJ-WHyMe v1. 3." *Geoscientific Model Development* 3: 565–584. https://doi.org/10.5194/gmd-3-565-2010.

West, W. E., J. J. Coloso, and S. E. Jones. 2012. "Effects of Algal and Terrestrial Carbon on Methane Production Rates and Methanogen Community Structure in a Temperate Lake Sediment." *Freshwater Biology* 57: 949–955. https://doi.org/10.1111/j.1365-2427.2012.02755.x.

West, W. E., K. P. Creamer, and S. E. Jones. 2016. "Productivity and Depth Regulate Lake Contributions to Atmospheric Methane." *Limnology and Oceanography* 61: S51–S61. https://doi.org/10.1002/lno.10247.

Wik, M., P. M. Crill, R. K. Varner, and D. Bastviken. 2013. "Multiyear Measurements of Ebullitive Methane Flux From Three Subarctic Lakes." *Journal of Geophysical Research – Biogeosciences* 118: 1307–1321. https://doi.org/10.1002/jgrg.20103.

Wilkinson, J., P. Bodmer, and A. Lorke. 2019. "Methane Dynamics and Thermal Response in Impoundments of the Rhine River, Germany." *Sci. Tot. Environ.* 659: 1045–1057. https://doi.org/10.1016/j.scitotenv.2018.12.424.

Wilkinson, J., C. Bors, F. Burgis, A. Lorke, and P. Bodmer. 2018. "Measuring CO_2 and CH_4 With a Portable Gas Analyzer: Closed-Loop Operation, Optimization and Assessment." *PLoS One* 13: e0193973. https://doi.org/10.1371/journal.pone.0193973.

Wilkinson, J., A. Maeck, Z. Alshboul, and A. Lorke. 2015. "Continuous Seasonal River Ebullition Measurements Linked to Sediment Methane Formation." *Environmental Science & Technology* 49: 13121–13129. https://doi.org/10.1021/acs.est.5b01525.

Wisser, D., S. Frolking, S. Hagen, and M. F. Bierkens. 2013. "Beyond Peak Reservoir Storage? A Global Estimate of Declining Water Storage Capacity in Large Reservoirs." *Water Resources Research* 49: 5732–5739. https://doi.org/10.1002/wrcr.20452.

Yvon-Durocher, G., A. P. Allen, D. Bastviken, et al. 2014. "Methane Fluxes Show Consistent Temperature Dependence across Microbial to Ecosystem Scales." *Nature* 507: 488–491. https://doi.org/10.1038/nature13164.

Zhu, Y., K. J. Purdy, A. Martínez Rodríguez, and M. Trimmer. 2023. "A Rationale for Higher Ratios of CH_4 to CO_2 Production in Warmer Anoxic Freshwater Sediments and Soils." *Limnology and Oceanography Letters* 8: 398–405. https://doi.org/10.1002/lol2.10327.

Zhuang, Q., M. Guo, J. M. Melack, et al. 2023. "Current and Future Global Lake Methane Emissions: A Process-Based Modeling Analysis." *Journal of Geophysical Research – Biogeosciences* 128: 2022JG007137. https://doi.org/10.1029/2022jg007137.

Zuur, A., E. Ieno, N. Walker, A. Saveliev, and G. Smith. 2009. Statistics for Biology and Health, Mixed Effects Models and Extensions in Ecology With R. New York: Springer. https://doi.org/10.1007/978-0-387-87458-6.

Supporting Information

Additional Supporting Information may be found in the online version of this article.

Submitted 15 April 2024
Revised 02 December 2024
Accepted 31 March 2025